Journal of Integrated
SCIENCE & TECHNOLOGY

Electrical behaviour of BaO-substituted multicomponent (K_2O-P_2O_5-Na_2O-CaO-B_2O_3) bioactive Glasses

Satish Khasa,* Rajesh Rohilla, Neetu Mann

Material Research Laboratory, Department of Physics, Deenbandhu Chhotu Ram University of Science & Technology, Murthal, India

Submitted on: 14-Jul-2024, Accepted and Published on: 05-Sep-2024

Article

ABSTRACT

Multicomponent glasses with composition *x*BaO-2K_2O-2P_2O_5-27Na_2O-21CaO- (48-*x*)B_2O_3 (*x* = 0, 2, 4, 6 & 8 mol%) has been prepared through melt–quench technique. X-ray diffraction (XRD), dielectric measurements, equivalent circuit analysis, *ac* and *dc* conductivity have been investigated. XRD profiles revealed that the produced samples were amorphous in nature. Dielectric parameters such as ε', ε'' and tanδ showed decreasing behaviour with rise in frequency. Nyquist plot attributed the relaxation to non-Debye type. The electric behavior of the samples was further studied using an equivalent circuit analysis corresponding to the Nyquist plot. The ac conductivity of prepared samples followed Jonscher's power law (JPL) and was observed to follow overlapping large polaron tunneling (OLPT) model. The semiconductor-like behaviour of the produced glasses is confirmed by the variation in dc conductivity with temperature. The dc conductivity results were analyzed using Arrhenius relation, which revealed high activation energies (> 1 eV) for all synthesized glasses and the Arrhenius plot's linearity is not deviated, which primarily illustrates the ionic conduction process.

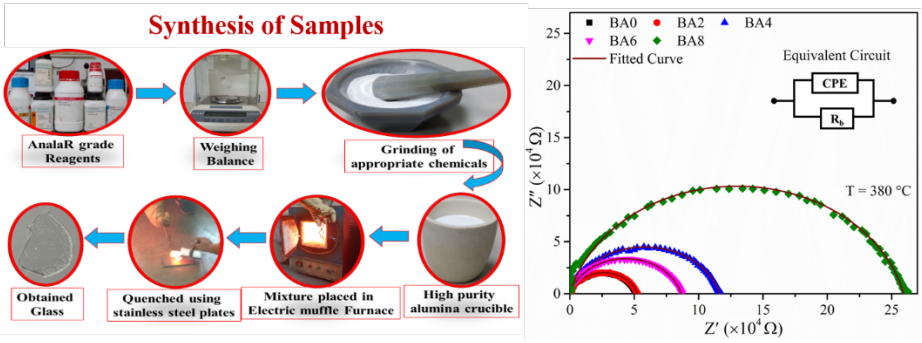

Keywords: Borate glass, Dielectric constant, Electric modulus, Nyquist plot, Jonscher's power law.

INTRODUCTION

Impedance spectroscopy is a very fruitful technique for analyzing the dielectric properties, relaxation process and conductive behaviour in glassy materials.[1,2] Borate-based glasses have gained considerable attention from past few years because of their ease of preparation, high bond strength, low cationic size, thermal stability and mostly used as a dielectric material which makes them promising candidate for technological applications.[3–5] Borate glasses are generally insulating in nature and are one of the most promising host matrices (good glass forming ability) for metal oxides such as alkali, alkaline or heavy metal oxides.[6] Addition of alkali metal ions (like as Na^+, Li^+, K^+ ions etc.) into borate-based glasses results in the enhancement of dielectric and electrical properties of the glasses. Further, to control the electrical conductivity of alkali-containing glasses, elements with large effective radius such as barium can be used to make them suitable for solid electrolytes in radiofrequency (RF) oscillators.[7] The controlled electrical conductivity property of glasses has gained significant scientific interest due to its potential applications as solid electrolytes in various electrochemical devices. These devices include smart windows sensors, chemical sensors, and high energy density batteries.[8] The conductive behaviour in these glasses may be due to ionic, electronic or mixture of ionic and electronic which depends on constituents and compositions of the glasses.[9] An extensive study of electrical properties of these glasses is therefore one of the main requirements to enable their use in aforementioned applications. To the best of our knowledge, there is less study on the electrical properties of barium doped borate-based glasses.

Motivated form aforementioned aspects, we synthesis BaO substituted in multicomponent K_2O-P_2O_5-Na_2O-CaO-B_2O_3 glass

*Corresponding Author: Prof. Satish Khasa, Department of Physics, Deenbandhu Chhotu Ram University of Science & Technology, Murthal, 131039, India
Tel: +919812818900; Email: skhasa.phy@dcrustm.org

Cite as: *J. Integr. Sci. Technol., 2025, 13(2), 1028.*
URN:NBN:sciencein.jist.2025.v13.1028
DOI:10.62110/sciencein.jist.2025.v13.1028

system. X-ray diffraction (XRD) is done to characterize the amorphous or crystalline nature of prepared glasses. In present study, BaO was replaced with B_2O_3 to explore the effect of BaO on alkali-containing borate-based glasses through investigation of dielectric properties and ac conductivity by using Impedance spectroscopy over a wide frequency and temperature range. The dc conductivity and activation energy of prepared glasses are also investigated using Arrhenius approach.

EXPERIMENTAL

Sample Preparation

Barium oxide containing alkali phospho-borate based glasses having composition xBaO-2K_2O-2P_2O_5-27Na_2O-21CaO- (48-x)B_2O_3 (x = 0, 2, 4, 6 & 8 mol% and encoded as BA0−8, respectively) were prepared by melt quench method [10]. Chemicals of analytical grade $BaCO_3$, K_2CO_3, P_2O_5, Na_2CO_3, $CaCO_3$ and H_3BO_3 were used to synthesize the samples. The started powdered chemicals were weighed on an electronic digital balance according to batch calculations and then thoroughly mixed using an agate pestle-mortar to get 15 g of a resulting homogeneous mixture. The resulting mixture was put in a high alumina crucible and subjected to melting at 1100 °C in an electric muffle furnace for 60 min. To ensure higher homogeneity, constant stirring of the mixture was done at regular intervals of 15 min. The melt was poured onto a preheated stainless-steel (SS) plate (at ~ 200 °C) and quenched by another SS plate to obtain the glass samples of uniform thickness. The glass slices were carefully obtained without any visible stria or bubbles and a portion of each sample was finely pulverised for XRD analysis. Glass samples were polished using emery paper and polished samples' surfaces were then coated with silver paste to get desired electrodes formation for both alternating current (*ac*) and direct current (*dc*) measurements.

Characterization

The XRD measurements of synthesized composition were conducted at room temperature (RT) with help of an X-ray diffractometer (Rigaku, Model: Ultima-IV). CuK_α radiation with a wavelength (λ) of 1.54 Å was employed, and the XRD instrument operated at a voltage of 40 kV and a current of 40 mA. An impedance Analyzer (LCR HiTester; Model: 3532-50 Hioki) was utilized to measure the dielectric characteristics with frequency variation from 100 Hz–5 MHz from RT to 380 °C temperature range. Keithley's source/measure equipment (Model 2401) was utilized to measure dc conductivity from RT to 380 °C temperature range.

RESULT AND DISCUSSIONS

X-ray Diffraction

Figure 1 portrays the XRD spectra of all prepared glass samples. From the spectra, it is observed that there are only broad humps in between 2θ = 20° and 35° and no crystalline phase exists and the absence of any sharp diffraction peak indicates the amorphous nature of prepared samples.[10] Additionally, it may be suggested that the introduction of BaO content do not affect the amorphous character of glass samples.

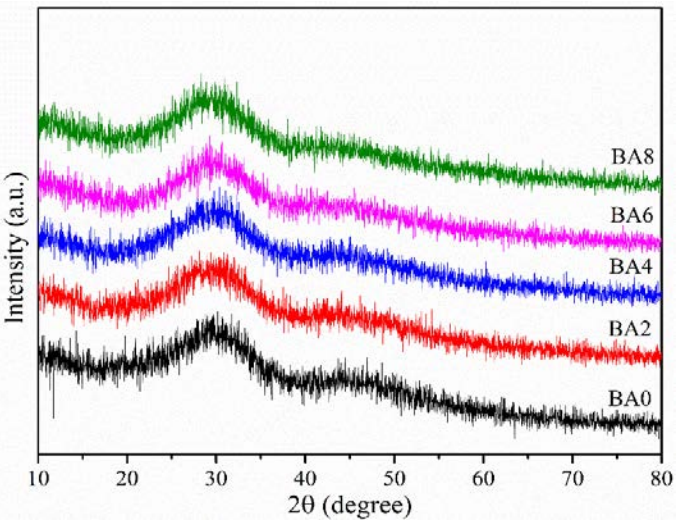

Figure 1. XRD patterns for BA0-8 glass system.

Dielectric properties

According to the dielectric properties, glass has two key electrical characteristics: first, it can act as an insulating medium with the ability in storage of electric charges and second, it can act as a conductive medium with the ability to transfer charge carriers.[11] When an electric field is applied corresponding to a dielectric substance, the amount of resistance is evaluated by permittivity measurements. Complex permittivity (ε*) is given by the following equation:

$$\varepsilon^* = \varepsilon' + i\varepsilon'' \qquad (1)$$

Where ε' is devoted to real parts of dielectric constant, which describe the polarizability, while ε'' is associated to imaginary parts of dielectric constant known as dielectric loss because of polarization. Investigation of the dielectric parameters of glasses over a wide frequency and temperature range aids to understand their performance under conditions of high temperature environment. Figures 2 (a) & (b) depict the variation in ε' *vs* frequency for BA0-8 glass system at 380 °C and for BA2 at various temperatures (300 °C – 380 °C), respectively.

It is observed from graphs that ε' shows dielectric dispersion having large values at low frequency domain and the values decrease rapidly with rise in frequency and become very small at high frequency domain. High values of ε' observed in the low frequency domain are possibly due to occurrence of accumulation of space charge at the interface of electrode. This accumulation hinders the further transfer of ions in the electrical circuit. Low values of ε′ at high frequency domain are possibly due to occurrence of periodic reversal of electric field which leads to a decrease in polarization and a reduction in accumulation of charge carriers.[12] In present study, it is found that the values of ε′ decrease with an increase in barium concentration which may be result of a barrier formation in the movement of Na^+ & K^+ ions due to Ba^{2+} ions. From Figure 2 (b), it is observed that in low frequency domain, variation in ε′ values are larger than that of high frequency domain as samples have barium ions do not have spontaneous polarization.

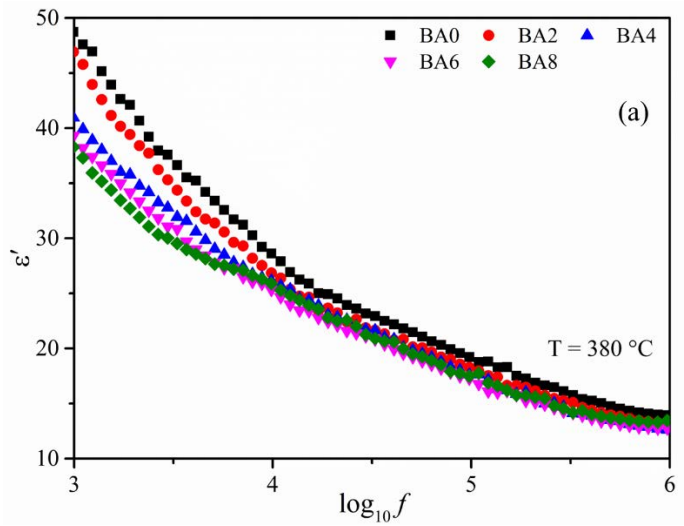

Figure 2 (a). Frequency dependence of ε′ for BA0–8 glass system at 380 °C.

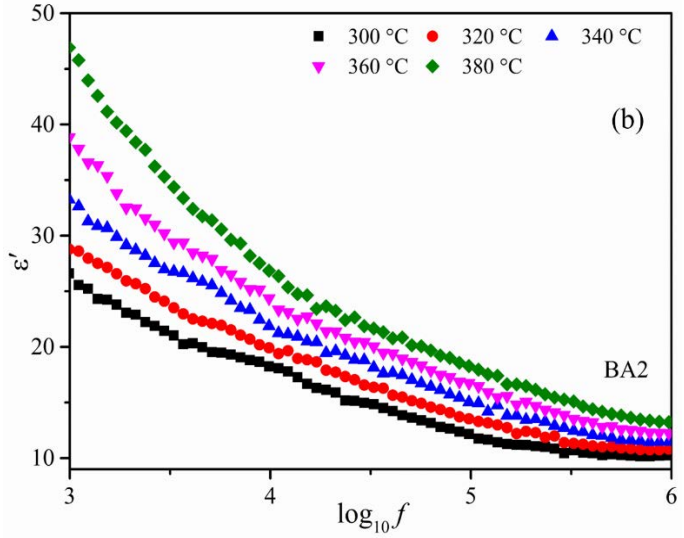

Figure 2 (b). Frequency dependence of ε′ for BA0 sample at various temperatures (300 °C – 380 °C).

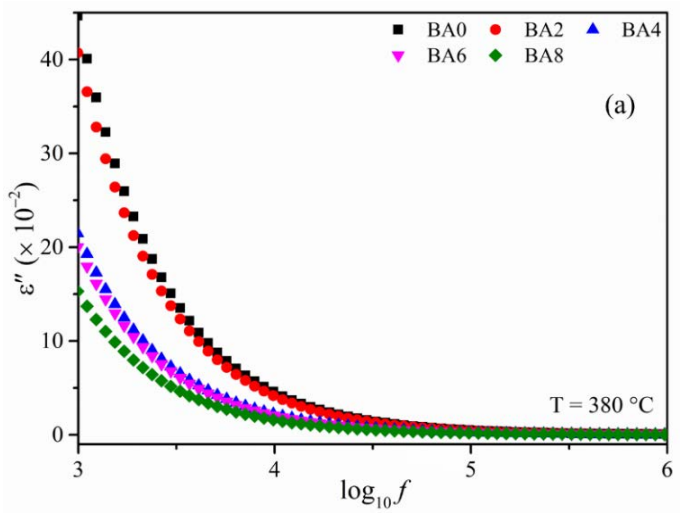

Figure 3 (a). Frequency dependence of ε″ for BA0–8 glass system at 380 °C.

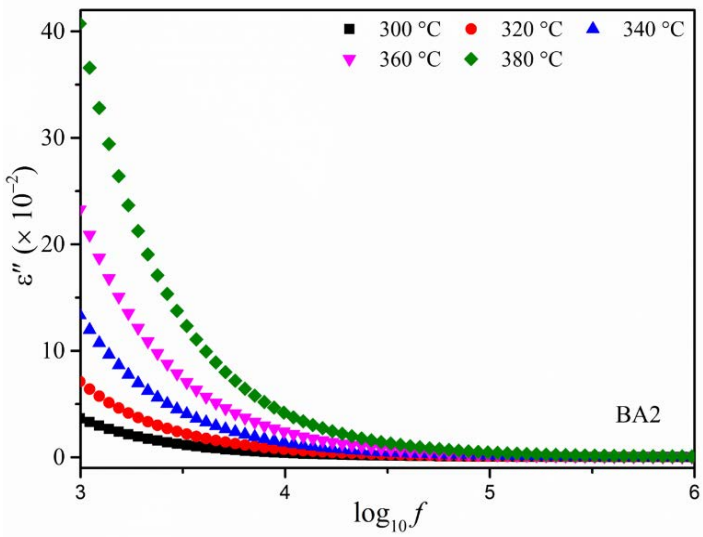

Figure 3 (b). Frequency dependence of ε″ for BA0 sample at various temperatures (300 °C – 380 °C).

With rise in temperature, separation of charge carries got disturbed because of thermal agitation and decrement in dipole formation which may result the expansion in glass network. Therefore, values of ε′ increase as a result of easier alignment of dipoles in field direction with rise in temperature.

When dielectric materials are exposed to a varying electric field, heat will be produced due to the reverse in polarity and shifting in dipoles, which is characterized as dielectric loss (ε").[13] Figures 3 (a) & (b) depict variation in ε″ with frequency for all prepared samples and for BA2 sample at different temperatures ranging from 300 °C to 380 °C.

The variation of ε″ values *vs* frequency shows similar trend as illustrated for ε′. The values of ε″ are observed to decline with rise in frequency which is possibly due to limited jumping frequencies of ions can match with frequencies of applied external field. The variation of ε″ values *vs* frequency shows a similar trend as illustrated for ε′. Therefore, individual dipoles have their own orientation and relaxation time. Further, conduction losses occur because of movement of charge carriers to large distances. These losses have minimum values at low temperatures and are proportional to ac conductivity of materials. In the movement of ions, some part of the energy may be transferring to lattice in form of heat. With increase in conductivity as rise in temperature, conduction loss increases which leads to an increment in dielectric loss.[14]

Loss Tangent

The loss tangent (tanδ) is well known as dissipating factor and is quantified due to small shift in practical performance corresponding to the ideal loss-free performance. This deviation occurs due to energy losses within a dielectric substance due to various relaxation processes. For better performance of a device, it is significantly to have less consumption of energy and low

dielectric loss, preferably across a wide range of operating temperature. The loss tangent (tanδ) can be expressed from relation:

$$tan\ \delta\ = \frac{\varepsilon''}{\varepsilon'} \qquad (2)$$

Figure 4 (a) & (b) show the frequency dependence of tanδ for all the synthesized glasses at 380 °C and for BA2 at various temperatures, respectively.

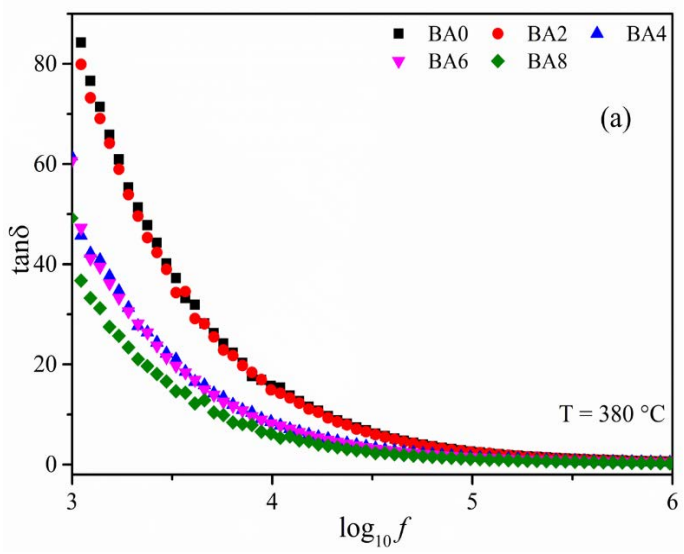

Figure 4 (a). Frequency dependence of tanδ for (a) BA0–8 glass system at 380 °C.

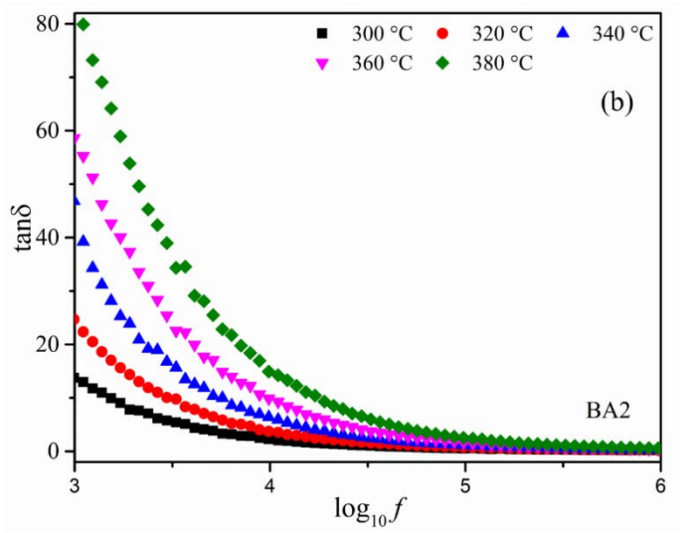

Figure 4 (b). Frequency dependence of tanδ for BA2 sample at various temperatures (300 °C – 380 °C).

The variation in values of tanδ with rise in frequency exhibits similar type of trend as observed in ε''. This can be explained due to the fact that contribution of polarizability from charge carriers decreases with rise in frequency and finally disappears due to inertia of the charges. At low frequency domain, values of tanδ are high due to space charge-polarization. At high frequency domain, alternating electric field changes so rapidly that charge carriers have less probability for diffusion, as a result of which charge accumulations get decreased [15] and therefore, decrease in values of tanδ is observed with rise in frequency. The low values of dielectric loss at high frequency domain exhibit that these prepared glasses are suitable for RF applications.[16]

Modulus Formalism

The electrical modulus (M*) formalism highlights the bulk features of interfacial polarization, which aids to understand the electrical relaxation behaviour of conductivity in materials [17]. The Electrical modulus (M*) is given by the formula:

$$M^* = \frac{1}{\varepsilon^*} = \frac{\varepsilon'}{\varepsilon'^2 + \varepsilon''^2} + i\,\frac{\varepsilon''}{\varepsilon'^2 + \varepsilon''^2} = M' + iM'' \qquad (3)$$

where M' & M'' are attributed to real and imaginary components of electrical modulus of the sample, respectively. Figures 5 (a) & (b) show the frequency-dependent variations of the real part (M′) and imaginary part (M″) of the dielectric modulus for the BA2 sample at different temperatures.

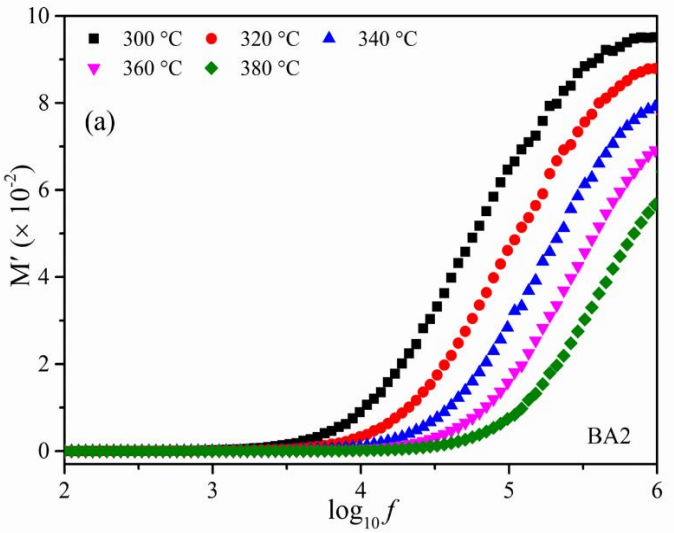

Figure 5 (a). Frequency dependence of the real part (M′) of the dielectric modulus for the BA2 glass sample across different temperatures, ranging from 300 °C to 380 °C.

At low frequency domain, M′ approaches to zero because of absence in restoring forces corresponding to mobile ions but dispersed with rise in frequency. The conduction mechanism in the dispersion region, at higher temperatures, is characterized by a shift towards higher frequencies, indicating the short-range mobility performance of charge carriers.

M′ began to saturate at a constant value towards the high frequency domain, establishing a plateau zone. On the other hand, spectra of M″ depicted a single relaxation peak that corresponded to dispersing region in M′. With rise in temperature, this peak is observed to shift towards high frequency domain. It suggests that mobility of charges is thermally activated. This rapid mobility of charges tends to decrease the relaxation time and therefore, relaxation mechanism depends upon temperature corresponding to rise in frequency.

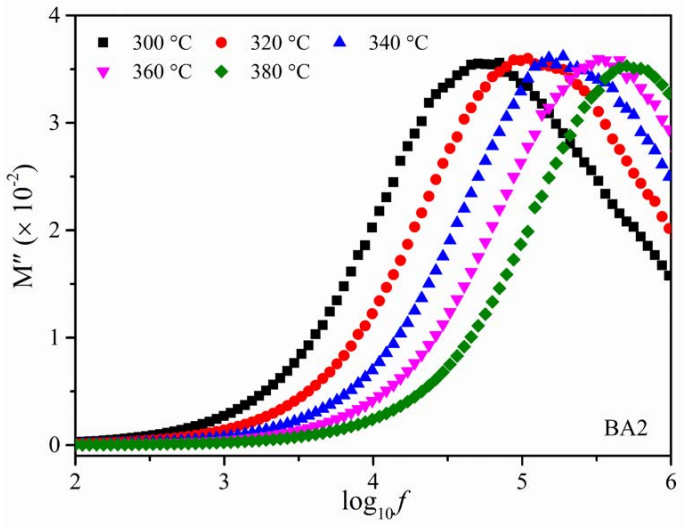

Figure 5 (b). Frequency dependence of the imaginary part (M″) of the dielectric modulus for the BA2 glass sample across different temperatures, ranging from 300 °C to 380 °C.

The distinctive peak in M″ also signifies a transition in the mobility of charges from long-range to short-range order. If frequency corresponding to highest value in the peak is abbreviated as f_{max}, then there are two possible outcomes that will be noted: (i) for frequency below f_{max}, movement of charge carriers can take place to long distances & (ii) for frequency above f_{max}, regular confinement of charge carriers in respective potential wells.[18] Therefore, broadening of peak suggested that different time constant have different relaxation time values, indicating non-Debye relaxation type.

Impedance spectroscopy

The impedance spectroscopy is a non-destructive tool to assess the electrical microstructure of glassy materials. It examines the impact of electrode polarization and grain boundaries on the electrical properties of the glasses. The relation that describes the complex impedance (Z*) is as follows:

$$Z^* = Z' + iZ'' \qquad (4)$$

Here Z′ represents the real part and Z″ represents the imaginary part. Nyquist plot is a graphical representation of the complex impedance between its real part (Z′) and imaginary part (Z″).[19] Figures 6 (a) & (b) shows the Nyquist plots for all synthesized samples at 380°C and for BA2 at different temperatures, respectively. The impedance data analysis reveals that there is an existence of single semi-circular arc in all synthesized glasses and single conduction mechanism is associated to these samples because of non- residual semicircles are observed at lower frequency.[6] The center of each semicircle in the Nyquist plot is observed to be compressed below the Z′ axis. This compression indicates that the relaxation of the associated ions follows a non-Debye type behavior.[20] The creation of non-polar clusters may be responsible for deviation from Debye to non-Debye nature in the prepared glass samples.

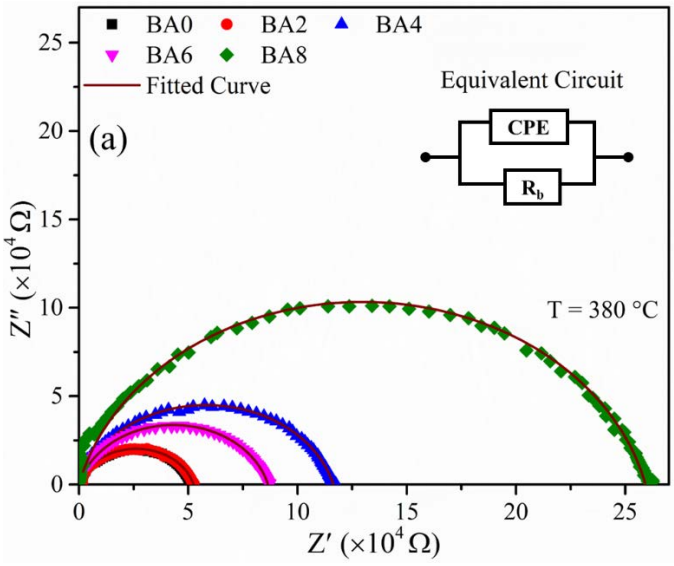

Figure 6 (a). Nyquist plots for BA0–8 glass system at 380 °C.

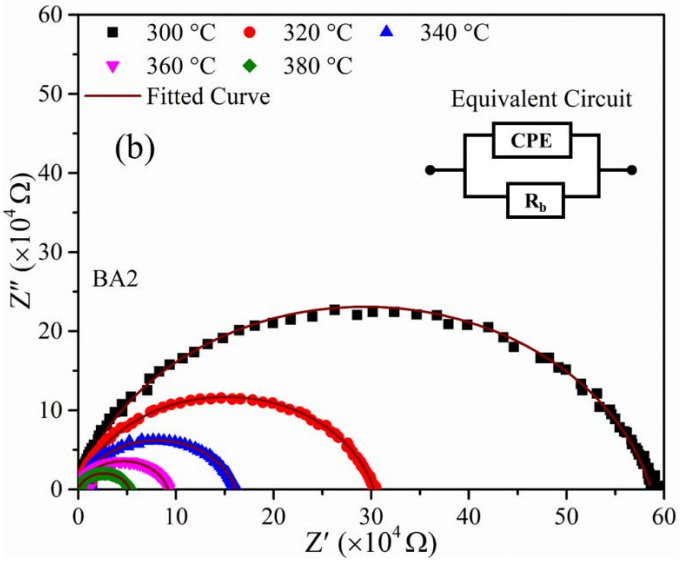

Figure 6 (b). Nyquist plots for BA2 at different temperatures (300 °C to 380 °C).

Equivalent Circuit Analysis

The experimental data is fitted to an equivalent circuit for impedance associated to combination of capacitors and resistors where capacitor represents space charge polarization on the electrodes, while resistors are attributed to bulk conductivity. It is suggested that depressed semicircles cannot be accurately fitted using an equivalent circuit consisting only of ideal capacitors and resistors. Therefore, to account for this non-Debye type behavior exhibited by the sample, a constant phase element (CPE) is introduced into the equivalent circuit instead of an ideal capacitor [15]. The inset of Figures 6(a) & (b) display the equivalent circuit as obtained from fitting of Nyquist data using EC–Lab V10.40 software. A good agreement is observed in fitted and experimental data. The equivalent circuit for fitted Nyquist data consists bulk

$$Z(f) = \frac{R_b}{R_b * (Q) * (i2\pi f)^{\alpha} + 1} \quad (5)$$

resistance (R_b) and *CPE* in parallel combination.[21] The equivalent circuit is fitted with the help of relation:

Where *Z*, α and Q are complex impedance, relaxation time distribution and constant phase element respectively.

Table 1 & 2 enlist fitted parameters from Nyquist plot for all synthesized glass samples at 380 °C and for BA2 sample at different temperatures (300 °C to 380 °C).

Table 1. Fitted parameters form Nyquist plot for BA0–8 glass system at 380 °C.

Parameters	BA0	BA2	BA4	BA6	BA8
R_b (*KΩ*)	51	52	116	86	259
C_1 (*pF*)	11.89	12.39	11.43	16.06	07.45
$Q * 10^{-10}$ ($F\ cm^{-2}\ s^{\alpha-1}$)	1.21	1.26	1.03	1.34	4.90
α	0.838	0.836	0.837	0.843	0.857

Table 2. Fitted parameters form Nyquist plot for BA2 at temperature range 300 °C to 380 °C.

Parameters	300°C	320°C	340°C	360°C	380°C
R_b (*KΩ*)	587	303	161	92	52
C_1 (*pF*)	11.99	12.05	12.14	12.13	12.32
$Q * 10^{-10}$ ($F\ cm^{-2}\ s^{\alpha-1}$)	0.72	0.92	1.05	1.05	1.26
α	0.849	0.838	0.836	0.842	0.836

Table 2, it is observed that values of R_b decrease as the temperature increases, suggesting the semiconductor type behaviour of synthesized samples. The amount of charge carriers in semiconductors that are responsible for conductivity normally rises as the temperature raises. From analysis, the intercept of the depressed semi- circular arcs on the Z′ axis at low frequency give the values of 'R_b' and decrease in resistance hike the conductivity of materials.

AC conductivity

Figures 7 (a) & (b) show the frequency dependence of ac conductivity (σ_{ac}) for BA0–8 samples at 380 °C and for BA2 sample in temperature range 300 °C to 380 °C, respectively. It is depicted from the graphs that at lower frequencies, σ_{ac} remains nearly constant and a plateau region is formed which may be attributed to significant contribution of bulk resistance, indicating the presence of space charge polarization effects. At the frequency increases, a dispersion region is observed which moves towards higher frequencies with rise in temperature. It can be observed from Figure 7 (a), σ_{ac} decreases with increase in BaO content, indicating the role of Ba^{2+} ions in creating a barrier in the pathway of Na^+ & K^+ ions. In other words, it may be suggested that BaO concentration controls the conductivity of the present glass composition.

From Figure 7 (b), it can be seen that values of σ_{ac} increase with rising temperature which can be attributed to the thermal activation of charge carriers.[22] The AC conductivity in glass samples can be described by Jonscher's power law (JPL) expressed as[23]:

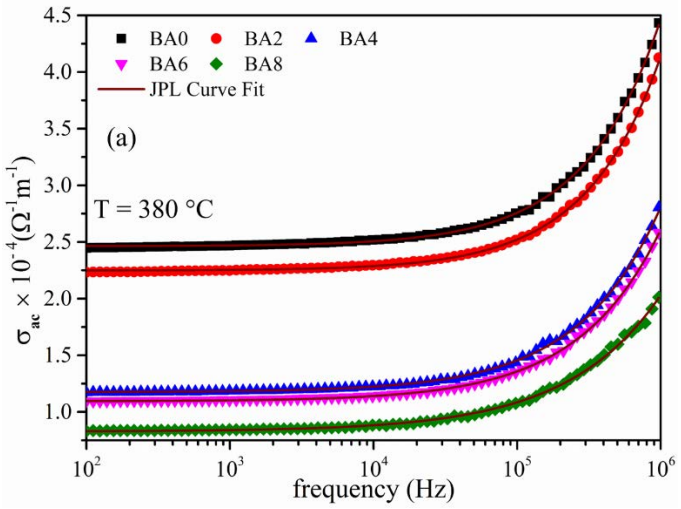

Figure 7 (a). σ_{ac} vs frequency plots for BA0–8 samples at 380 °C alongwith JPL curve fitting.

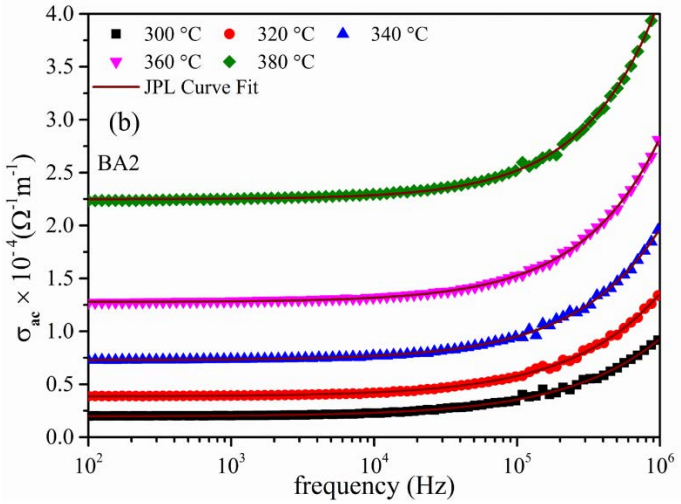

Figure 7 (b). σ_{ac} vs frequency plots for BA2 at different temperatures (300 °C to 380 °C) alongwith JPL curve fitting.

$$\sigma_{ac} = \sigma(0) + B\omega^{s} \quad (6)$$

Here σ (0), B and '*s*' represent frequency-independent conductivity, constant and power law exponent (also known as characteristic temperature dependent parameter), respectively. In general, '*s*' values fall inside the range of $0 < s < 1$ (calculated from JPL fitting of σ_{ac} *vs* frequency) and illustrate the degree of interaction with charges. The theoretically fitted curves for BA0-8 samples using JPL are shown in Figures 7 (a) & (b). The calculated values of ac conductivity alongwith corresponding parameters for all synthesized compositions at T = 380 °C and frequency 10 kHz are listed in Table 3.

Conductivity model

Figure 8 depicts the variation in 's' values with temperature plot for all studied glasses which are evaluated from the fitting the ac conductivity curves.

Table 3. AC and DC conductivity parameters for all prepared composition at 380 °C and f = 10 kHz.

Parameters	BA0	BA2	BA4	BA6	BA8
ε′	29.27	28.08	26.16	25.33	25.85
ε″	459.28	418.78	223.45	207.75	161.09
tan δ	15.69	14.91	08.54	08.20	06.23
σ_{ac} (×10^{-5}) (Ω^{-1}/m) (f = 10 kHz)	25.17	22.95	12.24	11.38	08.82
σ_{dc} (×10^{-5}) (Ω^{-1}/m)	09.04	10.79	08.55	08.01	06.59
Log σ_0	4.06	4.57	4.63	4.34	4.41
E_a (eV) For dc conductivity	1.05	1.11	1.13	1.10	1.12

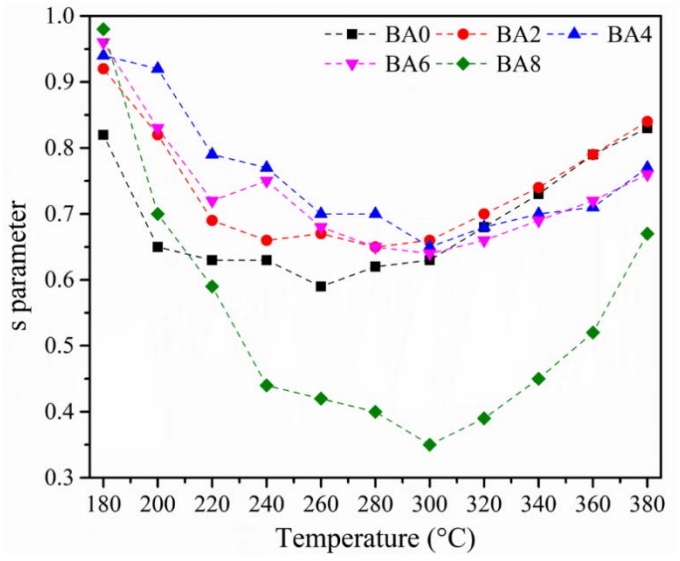

Figure 8. Variation of ‘s’ parameter with temperature for BA0–8 glass system.

The power law exponent (s) signifies kind of interaction in charge carriers which are responsible for conductivity. If value of ‘s’ is one, type of interaction will be considered as “Debye type interaction” i.e., there is no interaction between the charge carriers at all while for values of ‘s’ less than one, type of interaction will be considered as “non-Debye type interaction”. There are various theoretical models to predicted the conduction behaviour of materials, based on variation of ‘s’ with temperature. They include correlated barrier hopping (CBH), quantum mechanical tunneling (QMT), small polaron quantum mechanical tunneling (SPM) and overlapping large polaron tunneling (OLPT) model [24]. In these models, ‘s’ has distinct trends with frequency and temperature. According to QMT model, values of ‘s’ are predicted to be independent of temperature and conduction is because of phonons tunneling within defect states. In the CBH model, values of ‘s’ are predicted to be decrease with rise in temperature and conduction is because of transfer of charge carries between localized states over potential barrier. In the SPM model, values of ‘s’ rise with increase in temperature and conduction mechanism may be explained with quantum tunneling in small polarons. In the OLPT model, values of ‘s’ initially decrease thereafter increase with rise in temperature and conduction mechanism is based on overlap of large polarons due to their tunneling from potential wells [18]. Therefore, values of ‘s’ may play significant role in order to understand the conduction behaviour in present glass system corresponding to change in temperature. From Figure 8, it can be concluded that all prepared compositions complied with OLPT model.

DC Conductivity

Figure 9 (a) shows the variation in dc conductivity as a function of inverse of temperature for the synthesized compositions.

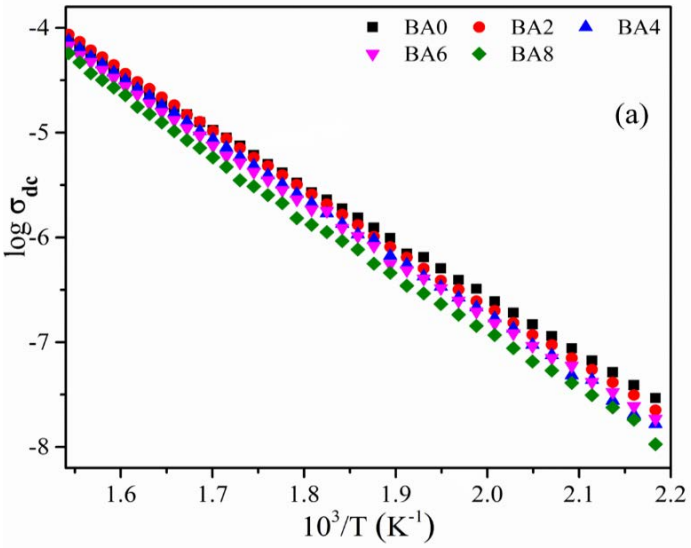

Figure 9 (a). Arrhenius plots corresponding to dc conductivity for BA0–8 glass system.

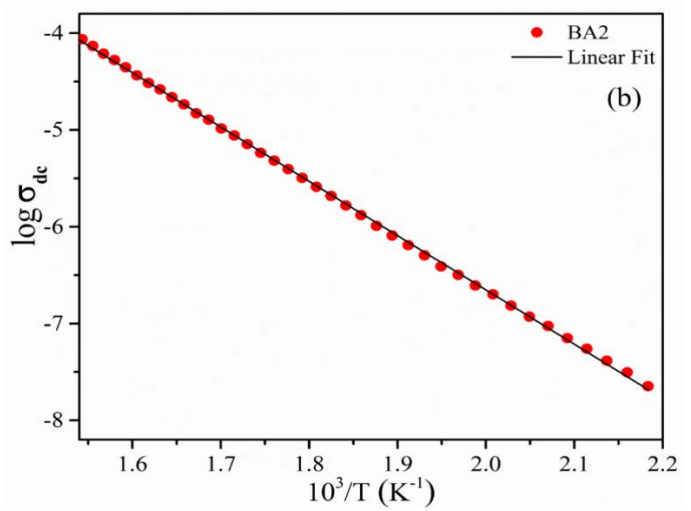

Figure 9 (b). Arrhenius plot corresponding to dc conductivity of BA2 sample alongwith linear fit space.

It is observed from graph that dc conductivity increases as the temperature rises. This observation suggests that the conduction mechanism is thermally triggered, indicating a semiconductor-like

behaviour of all prepared compositions. The dc conductivity values are observed of order 10^{-5} Ω^{-1}/m at 380 °C. The increase in values of dc conductivity with temperature can be explained by enhanced mobility of charge carriers with temperature results in increment of dc conductivity.[25] It can be depicted for the graph that dc conductivity (σ_{dc}) curve followed standard Arrhenius relation as[26]: Where E_a, k_B, T and σ_0 represent activation energy, Boltzmann constant, absolute temperature (in Kelvin) and pre-exponential factor. Table 3 enlists the values of σ_0 and E_a as evaluated by using

$$\sigma_{dc} = \sigma_0 exp\left(\frac{-E_a}{k_B T}\right) \quad (7)$$

intercept and slope of fitting Arrhenius plots, respectively; (as illustrated in Figure 9 (b) for BA2 sample). The values of E_a of synthesized compositions were found in the range of 1.05 to 1.13 eV. It is observed that addition of BaO increase the activation energy as compared to parent glass composition. High values of E_a and single sloped Arrhenius plot over the whole temperature range show the role of ionic conduction process due to migration of Na^+ & K^+ ions alongwith contribution of conduction due to heavy alkaline metal ions i.e., Ba^{2+} ions. As shown in Figure 9 (a), the dc conductivity of prepared samples decreases with increase in BaO concentration which may be due to formation of barrier by heavy alkaline metal Ba^{2+} ions in pathways of Na^+ & K^+ ions for ionic conduction.

Conclusion

Glasses having composition xBaO-2K_2O-2P_2O_5-27Na_2O-21CaO- (48-x)B_2O_3 (x = 0, 2, 4, 6 & 8 mol%) were synthesized successfully through melt-quench route. XRD patterns confirm the amorphous nature of prepared samples. The dielectric constant (ε'), dielectric loss (ε''), and loss tangent (tanδ) values were measured for the glasses at different frequencies and temperatures. It was observed that these values decreased at high frequency and increased with rising temperature. Low values of tanδ for high frequency domain suggested the synthesised samples were suitable for RF applications. The electrical modulus formalism was used to analyze the synthesized glasses, and it revealed the presence of a single relaxation phenomenon with non-Debye type behaviour.

Nyquist plots of all synthesized samples have shown the non-Debye relaxation behaviour and presence of a constant phase element (CPE). ac conductivity was found to decline with addition of BaO content and follow the JPL and governed by OLPT model. dc conductivity plots of all synthesized samples were found to follow Arrhenius equation. The conductivity results revealed that the above-synthesized glasses have potential applications for energy storage devices.

Acknowledgements

The authors express their gratitude to Department of Physics, DCRUST Murthal for providing access to XRD facility. Additionally, the authors would like to acknowledge the Department of Science & Technology (DST), Delhi for their experimental support through FIST Research Grant (SR/FST/PS-1/2018/32).

Conflict of Interest Statement

The authors declare no conflict of interest.

References

1. A. Yadav, M.S. Dahiya, P. Narwal, et al. Electrical characterization of lithium bismuth borate glasses containing cobalt/vanadium ions. *Solid State Ionics* **2017**, 312 (August), 21–31.
2. S. Khasa, M.S. Dahiya, A. Agarwal, P. Chand. EPR, FTIR, thermal and electrical properties of VO2+ doped BaCl2·BaO·B2O3 glasses. *J. Mol. Struct.* **2015**, 1079, 15–20.
3. H.I. Alkhammash, A.M. Ibrahim, S. Fouad. Enhancement of dielectric properties of borate glasses doped BaTiO3 for energy storage devices: characterization of optical, thermal and electrical properties. *J. Mater. Sci. Mater. Electron.* **2022**, 33 (21), 17048–17063.
4. R.A. Elsad, A.M. Abdel-Aziz, E.M. Ahmed, et al. FT-IR, ultrasonic and dielectric characteristics of neodymium (III)/ erbium (III) lead-borate glasses: experimental studies. *J. Mater. Res. Technol.* **2021**, 13, 1363–1373.
5. S.R. Rejisha, P.S. Anjana, N. Gopakumar. Effect of cerium(IV) oxide on the optical and dielectric properties of strontium bismuth borate glasses. *J. Mater. Sci. Mater. Electron.* **2016**, 27 (5), 5475–5482.
6. R. Rohilla, S. Khasa, A. Hooda. Structural and impedance spectroscopic investigations of eco-friendly alkali phosphoborate glass–ceramics containing zirconium ion. *Environ. Sci. Pollut. Res.* **2023**, 30 (44), 98609–98618.
7. G.H. Frischat. Mathematical approach to glass. byM. B. Volf. Elsevier Science Publishers, Amsterdam 1988. 420 pp., bound, DFL 275.-ISBN 0-444-98951-X. *Adv. Mater.* **1989**, 1 (6), 206–206.
8. N.S. Prabhu, K.R. Vighnesh, S. Bhardwaj, et al. Correlative exploration of structural and dielectric properties with Er2O3 addition in BaO–ZnO–LiF–B2O3 glasses. *J. Alloys Compd.* **2020**, 832, 154996.
9. M. Boora, S. Malik, V. Kumar, et al. Investigation of structural and impedance spectroscopic properties of borate glasses with high Li+ concentration. *Solid State Ionics* **2021**, 368 (June), 115704.
10. R. Rohilla, M.S. Dahiya, A. Hooda, A. Agarwal, S. Khasa. Effect of Li+ ions on structural, optical and nano-crystallization behaviour of Na2O-CaO- P2O5-B2O3 glass system: Biomedical applications. *J. Non. Cryst. Solids* **2022**, 593 (June), 121774.
11. S.N. Mohamed, M.K. Halimah, R.H.Y. Subban, A.K. Yahya. AC conductivity and dielectric properties in mixed ionic–electronic 20Na2O–20CaO–(60 – x)B2O3–xV2O5 glasses. *Phys. B Condens. Matter* **2021**, 602 (August 2020), 412480.
12. A. Langar, N. Sdiri, H. Elhouichet, M. Ferid. Conductivity and dielectric behavior of NaPO3–ZnO–V2O5 glasses. *J. Alloys Compd.* **2014**, 590, 380–387.
13. N. Kaur, G. Kaur, S. Khan, K. Singh. Conductivity, dielectric, and structural studies of (30-x) SrO-xBaO-10Al2O3-45SiO2-5B2O3-10Y2O3 ($5 \leq x \leq 25$) glasses. *Ionics (Kiel).* **2018**, 24 (8), 2343–2353.
14. M.S. Al-Buriahi, S. Alomairy, A. Saeed, A.S. Abouhaswa, Y.S. Rammah. Effect of ZrO2 addition on electrical and mechanical properties of B2O3–PbO–Li2O3 glasses. *Ceram. Int.* **2021**, 47 (9), 13065–13070.
15. J. Dahiya, A. Hooda, A. Agarwal, S. Khasa. Tuneable colour flexibility in Dy3+&Eu3+ co-doped lithium fluoride bismuth borate glass system for solid state lighting applications. *J. Non. Cryst. Solids* **2022**, 576 (October 2021), 121237.
16. R. V Barde, K.R. Nemade, S.A. Waghuley. Materials Science for Energy Technologies Impedance spectroscopy study of the AC conductivity of sodium superoxide nanoparticles doped vanadate based glasses. *Mater. Sci. Energy Technol.* **2021**, 4, 202–207.
17. A. Yadav, S. Khasa, A. Hooda, et al. EPR and impedance spectroscopic investigations on lithium bismuth borate glasses containing nickel and vanadium ions. *Spectrochim. Acta - Part A Mol. Biomol. Spectrosc.* **2016**, 157, 129–137.
18. M. Malik, S. Dagar, A. Hooda, A. Agarwal, S. Khasa. Effect of magnetic ion , Fe 3 + on the structural and dielectric properties of Oxychloro Bismuth Borate Glasses. *Solid State Sci.* **2020**, 110 (September), 106491.

19. S. Dagar, A. Hooda, S. Khasa, M. Malik. Rietveld re fi nement , dielectric and magnetic properties of NBT-Spinel ferrite composites. *J. Alloys Compd.* **2019**, 806, 737–752.
20. S. Dalal, S. Khasa, M.S. Dahiya, et al. Effect of substituting iron on structural, thermal and dielectric properties of lithium borate glasses. *Mater. Res. Bull.* **2015**, 70, 559–566.
21. R. Rohilla, S. Khasa, A. Hooda. In vitro study, structural and electrical characterization of alkali containing phosphoborate bioactive material. *Mater. Today Proc.* **2022**, 68 (xxxx), 139–145.
22. M.S. Dahiya, S. Khasa, A. Yadav, A. Agarwal. Appearance of small polaron hopping conduction in iron modified cobalt lithium bismuth borate glasses. *AIP Conf. Proc.* **2016**, 1731 (May), 3–6.
23. A.K. Jonscher. Dielectric relaxation in solids. *J. Phys. D. Appl. Phys.* **1999**, 32 (14), R57–R70.
24. S. Elliott. Frequency-dependent conductivity in ionic glasses: A possible model. *Solid State Ionics* **1988**, 27 (3), 131–149.
25. S. Dagar, A. Hooda, S. Khasa, M. Malik. Investigations of structural, enhanced dielectric and magnetic properties of NBT doped ferrite system. *Mater. Chem. Phys.* **2020**, 249 (May), 123214.
26. K.J. Laidler. The development of the Arrhenius equation. *J. Chem. Educ.* **1984**, 61 (6), 494.